Combining phase images from multi-channel RF coils using 3D phase offset maps derived from a dual-echo scan

S. Robinson[1], G. Grabner[1], S. Witoszynskyj[1], and S. Trattnig[1]
[1]Department of Radiology, Medical University of Vienna, Vienna, Austria

Introduction: Phase imaging is increasingly being used to provide alternative contrast in neuroimaging [1], to depict iron deposits in pathologies such as dementia, Huntington's, Alzheimer's and Parkinson's disease and to visualize vascular architecture in SWI. Phase imaging benefits from strong susceptibility effects at very high field and from the SNR and parallel imaging advantages offered by multi-channel coils. Phase images from a number of coils are optimally combined using complex sensitivity maps, derived from volume reference coil measurements [2]. There is currently no satisfactory method for combining phase images from multi-channel coils in the absence of a volume reference coil. The problem of phase image combination arises because each coil has a different phase offset, which varies over the object, reflecting the propagation distance to the coil. We present a method for calculating phase offsets via a weighted combination of phase measurements at two echo times, and using this information to combine phase data from a number of coils. The approach, Multi-Channel Phase Combination using measured 3D phase offsets (MCPC-3D), offers a conceptually and computationally simple solution to the calculation of combined phase images. The dual-echo data required for the phase offset maps can be intrinsic to the high resolution gradient-echo scan to be reconstructed (MCPC-3D-I), or may be acquired in a separate, fast, low resolution dual-echo scan (MCPC-3D-II). The quality of phase matching and phase images reconstructed with this method is assessed and compared with that achieved using rival reference-free methods; i) phase difference imaging, ii) unwrapping and phase filtering, and iii) a constant subtraction method.

Theory: The phase in coil *l,* for measurement *i* (of a multi-echo scan) is $\theta_{i,l}$ at time T_{Ei}, and is related to the local deviation from the static magnetic field, ΔB_0 (the source of image contrast), and the phase offset for that coil, $\theta_{RX,l}$ by Equ. 1 (neglecting phase wraps). A dual-echo scan in which the phase is measured at two echo times, T_{E1} and T_{E2}, allows $\theta_{RX,l}$ to be calculated via Equ. 2. Subtracting offsets from each channel allows a weighted mean phase, θ_{wm}, to be calculated over channels, Equ. 3, where M_l are the corresponding channel magnitudes.

Equations

$$1)\ \theta_{i,l} = 2\pi B_0 T_{Ei} + \theta_{RX,l} \qquad 2)\ \theta_{RX,l} = \frac{T_{E1}\theta_{2,l} - T_{E2}\theta_{1,l}}{T_{E1} - T_{E2}} \qquad 3)\ \theta_{wm} = \text{angle}\sum_l M_l e^{i(\theta_l - \theta_{RX,l})}$$

Materials and Methods: Measurements were made with a 7 Tesla MR whole body Siemens Magnetom scanner with a 24 channel Nova Medical RF coil. For MCPC-3D-I, an axial 3D, high resolution (0.3 mm in-plane resolution and 1.2 mm thick slices), dual-echo gradient-echo scan with TE/TR = (8, 15)/28 ms was acquired in 13 mins. A separate low resolution 2D dual-echo gradient-echo scan was acquired for the MCPC-3D-I method (applied to the second echo of the high resolution data set) with TE/TR = (4.6, 9.3)/606 ms, GRAPPA factor 4, TA = 27 s.

Analysis: The steps in MCPC-3D-I and MCPC-3D-II are illustrated in Fig. 1 and Fig. 2 respectively. Phase data at each echo time (Fig. 1-a, Fig. 2-b) were unwrapped in 2D using PHUN [3]. Phase offsets were calculated via Equ. 2 (Fig. 1-c, Fig. 2-d), and subtracted from individual channel data to yield well-matched data (Fig. 1-d, Fig. 2-e). These were combined using Equ. 3, and unwrapped (Fig. 1-f, Fig. 2-g). "Phase Difference" images were created using the Hermitian inner product method [4]. Separate channel data were unwrapped and high-pass filtered for the "Phase Filtering" method [5]. In the MCPC-C method (C='constant'), phase images were matched by subtraction of a scalar phase value, determined from the centre of each image [6]. For all methods other than Phase Filtering, images were high-pass filtered after unwrapping. As a measure of phase-matching quality, we examine the ratio of the magnitude of the complex sum vector divided by the sum of the individual vector magnitudes (which is close to 100% for well-matched phase data) for in-brain voxels (Fig. 3). Image GM-WM contrast to noise ratio was measured for each method.

Results: Phase matching was poor with MCPC-C (Fig. 3, brown line), and very good for the Phase Difference, Phase Filtering and MCPC-3D methods (Fig. 3). Phase image quality was poor with MCPC-C (Fig. 4), with complete signal cancellation in some regions (phase enlargement and arrow 1 in corresponding magnitude). Grey-white matter was low in the Phase Different method. Phase Filtering, MCPC-3D-I and MCPC-3D-II all yielded phase images with excellent GM-WM contrast (arrows 2 in Fig. 4), visualisation of small veins, and low noise. Of these three, MCPC-3D-II was the fastest to process, a factor 5 faster than the next fastest, Phase Filtering.

Figures:

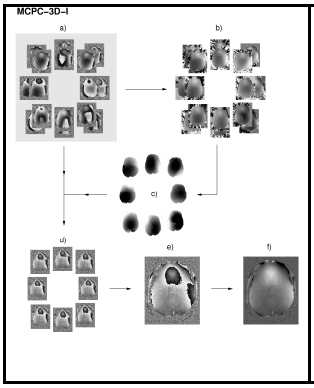

Fig.1: Steps in MCPC-3D-I

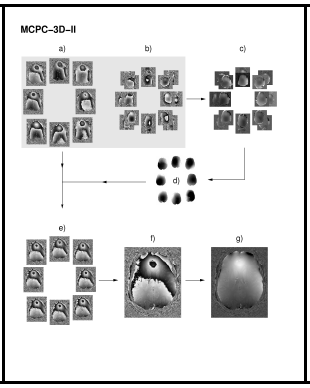

Fig.2: Steps in MCPC-3D-II

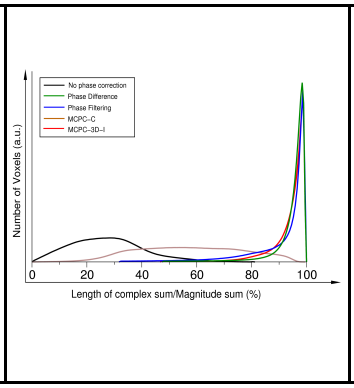

Fig.3: Quality of phase matching

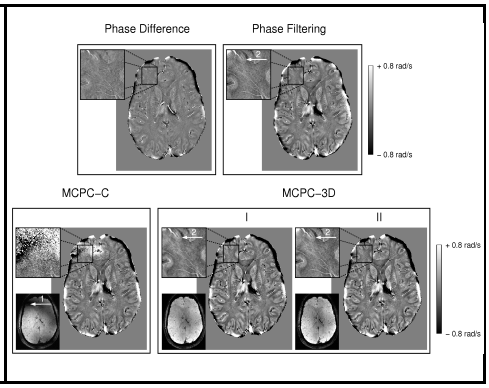

Fig.4: comparison of phase image quality

Discussion and conclusion: MCPC-3D is a conceptually simple and computationally undemanding approach to the calculation of combined phase images. Compared to current reference-free methods it yields images which have higher GM-WM CNR than MCPC-C and Phase Difference imaging. MCPC-3D-II is faster to process than the Phase Filtering (because only low resolution images need to be unwrapped) and requires no spatial filtering.

Acknowledgment: This study was funded, as part of the VIACLIC project, by the Vienna Spots of Excellence Program of the Centre of Innovation and Technology, City of Vienna (ZIT) and the Medical University of Vienna research grant AP00361OFF.

References: [1] Rauscher, A et al., (2005). Am J Neurorad; 26, 736-742. [2] Roemer PB et al., Magn Reson Med ; 16, 192-225. [3] Witoszynskyj, S et al., (2008). Med Im Anal; 13, 257-268. [4] Bernstein MA et al., (1994). Magn Reson Med ;32(3):330-334. [5] Koopmans PJ et al., (2008). Magn Reson Mater Phy ;21(1-2):149-158. [6] Hammond, KE et al., (2008). NeuroImage ;39, 1682 – 1692.